MÖSSBAUER SPECTROSCOPY--A REWARDING PROBE OF MORPHOLOGICAL STRUCTURE OF SEMICONDUCTING GLASSES

Punit Boolchand

Physics Department, University of Cincinnati

Cincinnati, Ohio 45221-0011

I. INTRODUCTION

It has been fashionable to discuss the structure of stoichiometric melt-quenched network glasses in terms of chemically-ordered continuous random networks (CRN) since Zachariasen's pioneering work on the subject nearly 50 years ago [1]. Glasses of the type AB_2, such as SiO_2 and $GeSe_2$ in analogy to a-Ge, for example, have been described as random networks of geometrically well-defined $A(B_{1/2})_4$ tetrahedral units.

The availability of new spectroscopic results in the past four years has shown, however, that the structure of these network glasses is not all that random. Specifically, Raman [2] and Mössbauer [3] experiments show that some fraction of like-atom bonds A-A and B-B appears to be an intrinsic feature of the completely relaxed stoichiometric melt-quenched $GeSe_2$ and GeS_2 glasses. The presence of a finite and reproducible broken chemical order and particularly its y composition dependence in $A_{1-y}B_{2+y}$ glasses (A=Ge, B=S or Se) indicates [3] that the microscopic origin of these like-atom bonds cannot be due to isolated bonding defects in a completely polymerized and chemically ordered $A(B_{1/2})_4$ network. These homopolar bonds appear to be clustered indicating, as we will show, a phase separation of the network on a molecular scale.

This new conceptual approach has been stimulated by the general recognition that although near-neighbor covalent bonding

forces are the most important forces contributing to the cohesive energy of a glass network, Van der Waals forces also play a significant role [4-6]. In chalcogen-based materials, Van der Waals forces derive from the resonance of lone pair electrons and these forces are known to promote chalcogen-chalcogen pairing as well as a tendency to form chain-like or ring-like or layer-like structures. That these forces must play a very special role in $GeSe_2$ glass may be seen from measurements [7] of molar volumes in the Ge_xSe_{1-x} binary which display a striking local maximum at the stoichiometric composition $x = 1/3$. These data underscore the importance of network packing forces (intercluster interaction) over covalent near-neighbor bonding forces (intracluster interaction) which lead to a low atomic density network for $GeSe_2$. One may understand why the lowest energy network configuration of a chalcogenide glass has a finite number of homopolar bonds in the following terms. Apparently, the loss in cohesive energy of a network upon forming a few percent of homopolar bonds is more than compensated by the increased Van der Waals contribution to this energy term upon promoting some chalcogen-chalcogen pairing [6].

To quantitatively understand the observation of broken chemical order, it has been suggested [6] that these $GeSe_2$ and GeS_2 glasses consist of at least two types of morphologically and stoichiometrically distinct large molecular clusters, analogous to donor and acceptor molecules in molecular crystals. In this molecular cluster network model (MCN) approach, cluster surfaces are believed to play an integral role in determining the glass-forming tendency. In this approach, the degree of broken chemical order is derived from the surface to volume ratio, namely, the size of the clusters. In this review, we will highlight some new experimental developments that shed light on the idea of molecular clustering in network glasses. These new experimental developments have utilized Mössbauer spectroscopy [8] as a probe of chemical order of both anion and cation sites in the present glasses.

Broadly speaking, several thousands of experiments on the micro-molecular structure have utilized one of the four general probes listed in Table I. The methods falling in categories I, II, and III, namely, diffraction methods [10], vibrational spectroscopy [11], and photo-emission spectroscopy [12], have been reviewed in the literature from time to time. Mössbauer spectroscopy as a probe of network structure of semiconducting glasses forms the scope of the present review. Two previous reviews on the current subject, one by P.P. Seregin et al. [8] and the other by

Table I. Experimental methods of studying the structure of inorganic glasses.

	Method	Experimental Observable	Connection With Structure
I.	Diffraction		
(a)	e,n, X-ray diffuse scattering	Structure Factor	Pair Correlation Function;
(b)	EXAFS	Interference Function	Coordination number and
(c)	XANES		bond lengths of near-
(d)	SANS		neighbors
II.	Vibrational Spectroscopy		
	Infrared	Normal modes of	Identify building blocks of
	Raman	characteristic building	a network glass
	Mossbauer	blocks	
III.	Photoelectron Spectroscopy		
	X-ray Photoemission	Density of electron-	Ring statistics of network
	UV Photoemission	valence or core states	
IV.	Hyperfine Interactions		
(a)	NQR (Nuclear Quadrupole Resonance)	EFG, Relaxation times	Local bonding chemistry
(b)	NMR (Nuclear Magnetic Resonance)	Chemical shifts	
(c)	μSR (Muon Spin Resonance)	Chemical shifts	
(d)	ME (Mössbauer Effect)	EFG, $\lvert\psi(o)\rvert^2$ contact charge density	
(e)	TDPAC (Time-Dependent Perturbed Angular Correlation)	EFG	

W. Müller-Warmuth and H. Eckert [8], appeared nearly two years ago. For completeness, it may be also mentioned that Mössbauer spectroscopy has been widely utilized to characterize Fe sites in a variety of metallic as well as insulating glasses [9]. Some of the other site spectroscopies, particularly NMR [13] and NQR [14], as probes of structure in glasses are well documented.

Our presentation in this review is as follows: In Section II, we provide some background material on Mössbauer spectroscopy. The intention is to familiarize the reader with the method, thus making easier the interpretation of the spectra of chalcogenide network glasses. In Section III, we present experimental results on g-$GeSe_2$, first as revealed by diffraction measurements and vibrational spectroscopy, and then as extended by the present Mössbauer results. Instead of describing results on a variety of glass systems, we have thus chosen to focus on g-$GeSe_2$. This approach will permit not only illustration of the application of the present method but also a complete structure discussion of the prototypical glass. We conclude our illustrative review with some cautionary general remarks on the scope and limitations of the present method in Section V, where we also summarize our conclusions.

II. MÖSSBAUER SPECTROSCOPY

Neither Se nor Ge [15] offers the prospect of a suitable Mössbauer probe for glass work. The heavier isovalents of these elements, namely, Te and Sn, have, however, suitable Mössbauer resonances. The experimental approach, therefore, requires that ternary alloys of Ge, Se and Sn or Ge, Se and Te be investigated, and this is a point we will return to later. Upon alloying trace amounts of Sn or Te in $GeSe_2$ glass, one can expect these impurity atoms to mimic respectively the bonding chemistry of the cation and anion sites provided no phase separation occurs. In this section, we introduce the method focussing principally on ^{119}Sn absorption (probe of cation sites) and ^{129}I emission (probe of anion sites) spectroscopy. We have taken examples out of our glass work to illustrate the principles of the method. Excellent review articles on various aspects of the spectroscopy are available in the literature [16].

The principal components of a Mössbauer spectrometer are shown in Fig. 1, and consist of a velocity drive (transducer), an emitter attached to the drive, an absorber that is stationary, and a low energy x-ray detector. To display the lineshape of the nuclear

resonance, one records the transmission of γ-rays through an absorber as a function of energy of the emitted γ-rays. The latter is accomplished using the Doppler effect. By imparting a precise velocity either positive (motion toward absorber) or negative (motion away from absorber), one increases or decreases the energy of the emitted γ-ray (E_γ) as seen in the frame of reference of the stationary absorber. Constant acceleration drives used in conjunction with multichannel analysers permit one to continuously scan a velocity range, i.e., a narrow energy window $\pm \frac{v}{c} E_\gamma$ centered around the emission line, and observe the resonance lineshape directly. Because of the recoil-free nature of the effect,

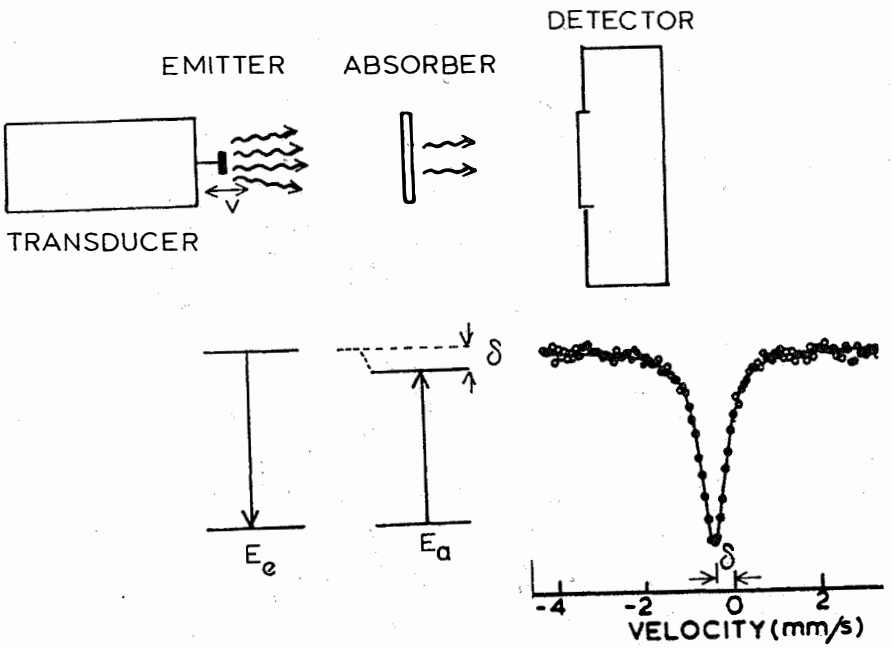

Fig. 1 Elements of a Mossbauer spectrometer: Transducer, emitter, absorber, and detector. Shown below the experimental arrangement is the nuclear level splitting. If the gamma ray energy in the emitter (E_e) exceeds the transition energy in the absorber (E_a) by an amount δ, the resonance centroid will be observed at a negative Doppler velocity.

the linewidth of the nuclear resonance is the natural width given by Heisenberg's uncertainty principle. The linewidth ($2\hbar/\tau$) is determined by the lifetime (τ) of the nuclear excited state and this width is typically of the order of 10^{-7}eV. This linewidth translates into a Doppler velocity which is usually a fraction of a mm/s. Figure 2 shows a spectra of some Sn-bearing crystals taken with such a spectrometer.

There are basically three pieces of information that can be obtained from an analysis of the spectra shown in Fig. 2. This information is derived from:

(a) Lineshift
(b) Line-shape or splitting
(c) Integrated intensity

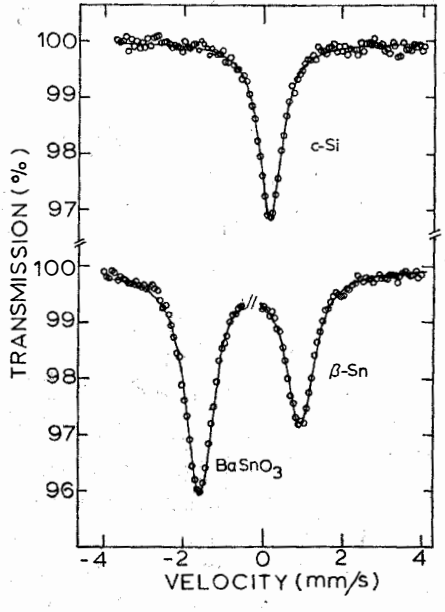

Fig. 2 ^{119}Sn spectra of indicated absorbers taken with an emitter of $^{119}Sn^{m}$ in vanadium metal. Lineshifts of c-Si and β-Sn relative to $BaSnO_3$ are plotted in Fig. 3.

These experimental observables permit one to microscopically characterize the chemical environments of the probe atoms either in the emitter or in the absorber matrix. The chief utility of this spectroscopy derives from the fact that the strength of hyperfine interactions (i.e., lineshift and linesplitting) usually is larger than the natural linewidth of the nuclear resonance, enough to permit separation of signals from different sites.

A. Probe of Ge Sites in Network Glasses

In favorable cases, one may hope to isolate the chemical bonding configuration of Ge sites in a network glass by alloying traces of Sn and pursuing ^{119}Sn absorption measurements. In such measurements, the spectrum of a Sn-bearing glass or crystal, used as an absorber, is taken with a mono-energetic emitter of the 23.8keV γ-ray ($3/2 \rightarrow 1/2$ transition). The absorption spectra of indicated hosts shown in Fig. 2 were taken with a source of 250 days $^{119}Sn^{m}$ diffused in vanadium metal.

The location of the absorption line on the velocity axis measured in relation to some standard host is known as the isomer-shift or lineshift. The standard host taken for this purpose include either $BaSnO_3$ or $CaSnO_3$. Both these materials are examples of Sn^{4+}, and show a narrow line whose center of gravity is the same. As can be seen from Fig. 2, the shifts of β-Sn and c-Si are both positive and approximately 2.5mm/s and 1.7mm/s, respectively. These shifts in energy units directly provide the difference in transition energy of the 23.8keV γ-ray in various hosts. Specifically, the spectra of Fig. 2 show that the transition energy in $BaSnO_3$ to be the smallest while that in β-Sn is the largest.

The isomer shift δ is generally written as

$$\delta = \frac{2\pi}{5} Ze^2 \Delta\langle r^2\rangle \left[|\psi(o)|^2 - |\psi(o)|^2_{ref}\right]. \qquad (1)$$

The term in square brackets represents the electron charge density at the nuclear site in the host of interest measured relative to the reference host. In Eq. (1), $\Delta\langle r^2\rangle$ represents the change in the nuclear charge radius between the ground and excited state, and this nuclear moment has been established [16] to be $+3.3 \times 10^{-3}$fm^2 for ^{119}Sn.

Figure 3 gives a ^{119}Sn isomer shift scale in which we have projected shifts of selected Sn bearing crystals as well as glasses. On this plot, we find that shifts characteristic of tetrahedral Sn

reside in the region of +1.3mm/s to +2.0mm/s, a region which lies in-between the shifts of Sn^{4+} and Sn^{2+}. The large positive shifts of Sn^{2+} can be understood in terms of the two 5s-like valence electrons that are localized on Sn. These contribute overwhelmingly to the contact charge density $|\psi(o)|^2$. Just the reverse is true for Sn^{4+}, which has the lowest $|\psi(o)|^2$ because of the absence of these 5s electrons. Sn present in a local tetrahedral symmetry, as in c-Si, is described in terms of sp^3-like covalent bonds. This configuration has a shift that resides in-between Sn^{4+} and Sn^{2+}, primarily because only one 5s-like electron contributes to $|\psi(o)|^2$.

α-Sn and Sn as an impurity in the group IV elemental semiconductors [17] represent some of the few examples of tetrahedrally coordinated species found in crystalline hosts. Because of its more metallic character, Sn tends to choose octahedral over tetrahedral coordination in most Sn-bearing crystals. In covalent glasses, which are less dense than their crystalline analogues, just the reverse is true, and we find, for example, that Sn is predominantly tetrahedral in GeX_2 glasses (X=S, Se, and Te). As discussed later, spectra of these glasses display an intense Sn

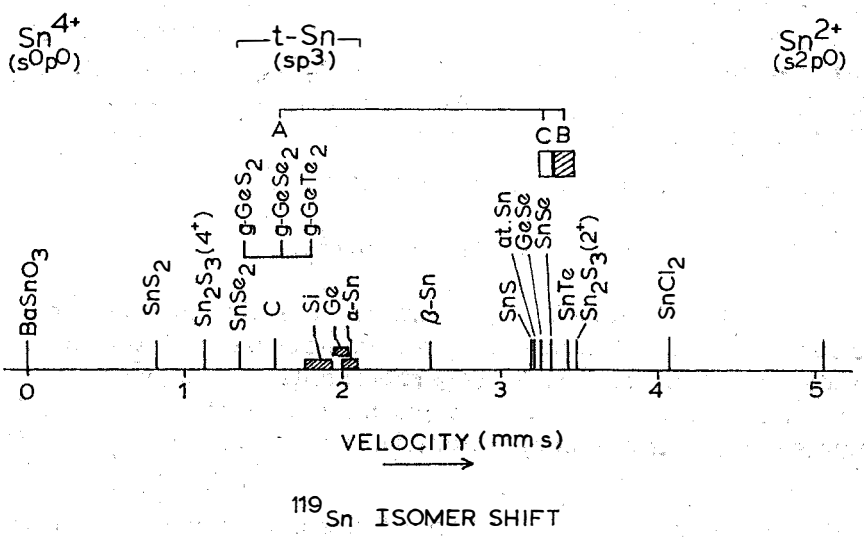

Fig. 3 ^{119}Sn isomer shifts of selected crystals and chalcogenide glasses.

site (usually labelled as A site) characterized by a narrow line. We have found [18] that if one plots the lineshifts of these A sites and the shifts of several Sn tetrahalides where the cation is known to be fourfold coordinated in a tetrahedral symmetry, against the Pauling electronegativity difference $\Delta\chi_P = \chi_X - \chi_{Sn}$, then a universal correlation results (Fig. 4). We have shown elsewhere [18] that this correlation can be quantitatively understood in terms of covalently bonded interactions which are modified by charge transfer effects. This correlation serves as conclusive evidence that the A sites seen in the GeX_2 glasses represent geometrically and chemically tetrahedrally coordinated Sn species. This is a point that has largely gone unappreciated by Soviet workers in the field (see P.P. Seregin et al in ref. 8) who have in our view erroneously ascribed this site A to Sn^{4+}, an octahedrally coordinated species, as found in corresponding crystals.

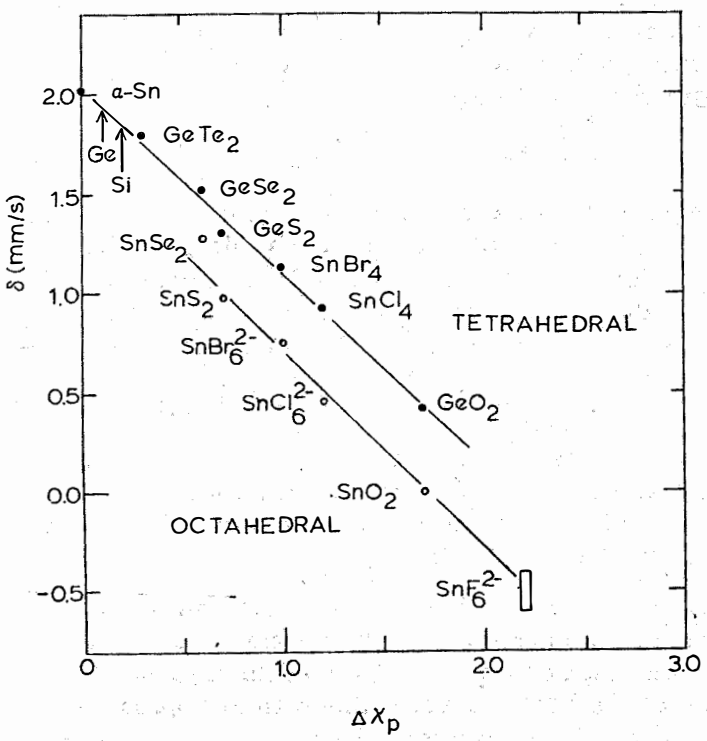

Fig. 4 ^{119}Sn isomer shifts of SnX_4 tetrahedral species plotted as a function of Pauling electronegativity difference $\Delta\chi_P = \chi_X - \chi_{Sn}$. Figure is reproduced from ref. 18.

The isomer shift of Sn^{2+} species in covalent networks usually tends to be in the vicinity of 2.9mm/s to 3.4mm/s and furthermore is correlated with the quadrupole splitting that invariably accompanies such species. This correlation has been discussed by a number of previous workers in the field and the reader is referred to ref. [19] for a more complete discussion.

(i) Line Splitting

It is usual not to observe single lines but a multiplet structure when probe atoms reside in a host that is magnetic and/or noncubic. The origin of this multiplet structure can be traced to either an electric quadrupolar and/or magnetic dipolar interaction which may be static or dynamic in origin. Specifically, when probe atoms occupy sites of noncubic local symmetry, the presence of an Electric Field Gradient (EFG) tensor leads to a splitting of the resonance line into a multiplet. In ^{119}Sn spectroscopy, this multiplet consists of a doublet which arises due to the presence of an electric quadrupole interaction in the $3/2^+$ 23.8keV state (Fig. 5), given by the relation

$$\Delta = \frac{e^2 Q V_{zz}}{2} (1 + \eta^2/3)^{1/2} \qquad (2)$$

where eQ = -0.065 barns is the nuclear quadrupole amount of the $3/2^+$ states [16]. In insulating and covalent networks, which may be crystalline or glassy, the principal contribution to the EFG (eV_{zz}) arises due to an imbalance of the atomic-like 5p charge cloud of Sn and one can write the EFG as follows:

$$eV_{zz} = -\frac{4e}{5\langle r^3 \rangle} \left[U_z - \frac{U_x + U_y}{2} \right] (1+R) \qquad (3)$$

where $U_{x,y,z}$ denote the population of the p_x, p_y, and p_z orbitals, while R represents the Sterheimer shielding factor [20]. The EFG physically provides a measure of the asphericity of the charge distribution about probe nuclear sites.

A second source of EFG arises due to charges external to probe atoms and in crystals of high symmetry (such as hexagonal) lattice sum calculations have been used to estimate this host contribution of the EFG. Several theoretical approaches have been used to estimate EFG in disordered solids. In conducting glasses which are described in terms of closed packed structures, distribution of EFG parameters has been estimated for the case of dense random packing [21]. In semiconducting glasses, an atom-

istic approach [22] (extended Huckel procedure) and also a band approach [22] has been used to calculate EFGs. It is beyond the scope of this review to discuss these approaches in any detail.

(ii) Integrated Intensity

Information pertaining to atomic dynamics of probe atoms is contained in the area under the resonance line. Specifically, temperature variation of the integrated intensity provides a means to obtain the mean square displacement of the probe atoms. In glasses, this can be related to specific low frequency vibrational modes in the one phonon density of states. Mossbauer spectroscopy can, thus, serve as a chemically specific vibrational spectroscopy.

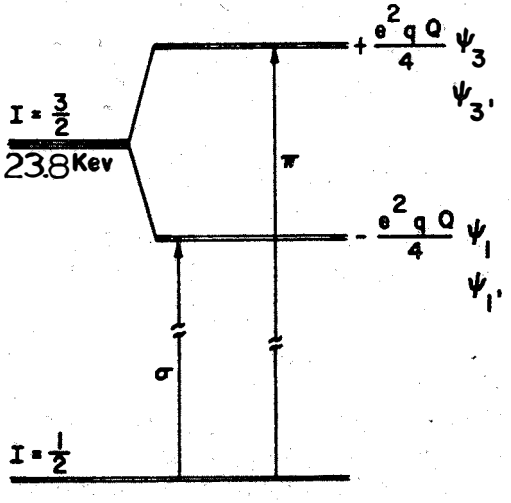

Fig. 5 Doublet spectra in ^{119}Sn spectroscopy usually result due to an electric quadrupole interaction in the $3/2^+$ nuclear state. When the EFG is axially symmetric ($\eta=0$), the π ($\pm 1/2 \rightarrow \pm 3/2$) and σ ($\pm 1/2 \rightarrow \pm 1/2$) are pure transitions.

(iii) Multiple Line (Site) Intensity Ratios

In instances when a spectrum yields multiple sites that are chemically inequivalent, Mossbauer spectroscopy provides a means to establish directly the relative population of these sites by comparing the ratio of the areas under respective multiplet structures. In glasses, site intensity ratios have proved to be a powerful probe of network morphology [3,23], as we shall demonstrate by some examples in the present work.

B. Probe of Chalcogen Sites in Network Glasses

It is possible to probe the chemistry of chalcogen sites in crystals or glasses by using the 35.5keV ($3/2^+ \rightarrow 1/2^+$) γ-resonance in ^{125}Te in absorption spectroscopy, or the 27.8keV ($5/2^+ \rightarrow 7/2^+$) in ^{129}I, using emission spectroscopy [24]. In the latter approach, the glass of interest forms the emitter matrix and its spectrum is taken with a monoenergetic absorber. There are several advantages to using the latter approach.

1. The ^{129}I resonance offers an order of magnitude greater resolution than the ^{125}Te resonance because of its narrower natural linewidth (0.69mm/s versus 5.2mm/s).

2. Second, because the quadrupole moments of the nuclear states in ^{129}I are a factor of approximately three larger [16] than in ^{125}Te, one has greater sensitivity. One can probe, for example, all other things being equal, smaller EFGs.

3. In emission spectroscopy, a change in chemistry occurs on going from a Te parent atom to an I daughter atom which considerably simplifies the microscopic interpretation of the NQI parameters. Ths simplification can be traced to the tendency of I to be onefold coordinated and is a point we shall return to later.

The chief disadvantage of this method is that the noncrystalline host of interest has to be labelled by ^{129}Te^m atoms (radioactive). While this is not a problem in working with bulk glasses, this does pose difficulties in examining sputtered or evaporated samples unless provision for ion implantation exist [25], in which case, the probe atoms can be implanted after the fact of sample preparation.

In practice, one can combine both absorption and emission spectroscopies to gain insights in the chemistry of the chalcogen site in covalent network glasses. We have used both approaches

to investigate in detail melt-quenched $GeSe_{2-x}Te_x$ ternary glasses. In Section III, we shall describe results obtained from ^{129}I emission spectroscopy on this ternary. The reader is referred to ref. [26] for discussion of the ^{125}Te absorption spectroscopy results on this system.

The central idea of ^{129}I emission spectroscopy is that one infers the bonding chemistry of parent $^{129}Te^m$ atoms (usually alloyed or implanted) in the chalcogen-based host by measuring the nuclear hyperfine structure of the daughter ^{129}I atoms that are formed by nuclear transmutation (β-decay). In this approach, the matrix of interest is the emitter matrix and one records its spectrum with a monoenergetic ^{129}I absorber, which is usually taken to be cubic NaI. This is convenient because the latter host which contains I in a closed shell configuration (I^-) is also used as a reference [27] for isomer-shifts measurements.

In instances when ^{129}I probe atoms are present in a locally noncubic environment, one observes a 12 line multiplet structure arising out of a NQI in both the $5/2^+$ ground and $7/2^+$ excited state as shown in Fig. 6. The multiplet structure can be theoretically

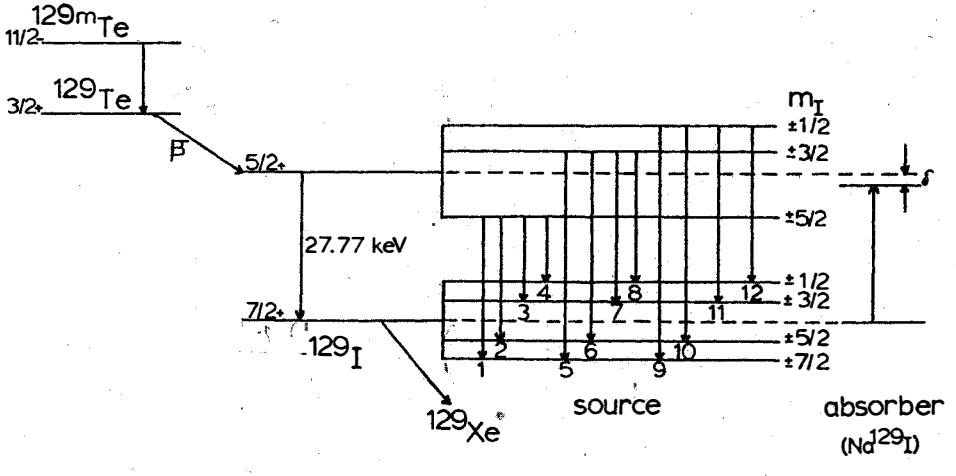

Fig. 6 Electric quadrupole interaction in the $7/2^+$ and $5/2^+$ state of ^{129}I showing the 12 transitions that result on account of the mixed (MI + E2) nature of the 27.77keV γ-transition.

analyzed in terms of 3 parameters: a centroid or isomer shift (δ), ($e^2Q_gV_{zz}$), nuclear quadrupole coupling in the ground state and $\eta = |V_{xx} - V_{yy})/V_{zz}|$, the asymmetry parameter of the EFG tensor. The nuclear quadrupole moment ratio R (= Q_e/Q_g) of the excited (Q_e) to ground state (Q_g) has been established [28] to be 1.238(1). In Fig. 7, we show the η dependence of the multiplet structure for a fixed $e^2Q_gV_{zz}$ value, and note that generally the hyperfine structure yields a pattern that lacks inversion symmetry about its centroid. This has the important consequence that the sign of the quadrupole coupling constant, and therefore the EFG, can be uniquely established from such a spectrum. Only for the case

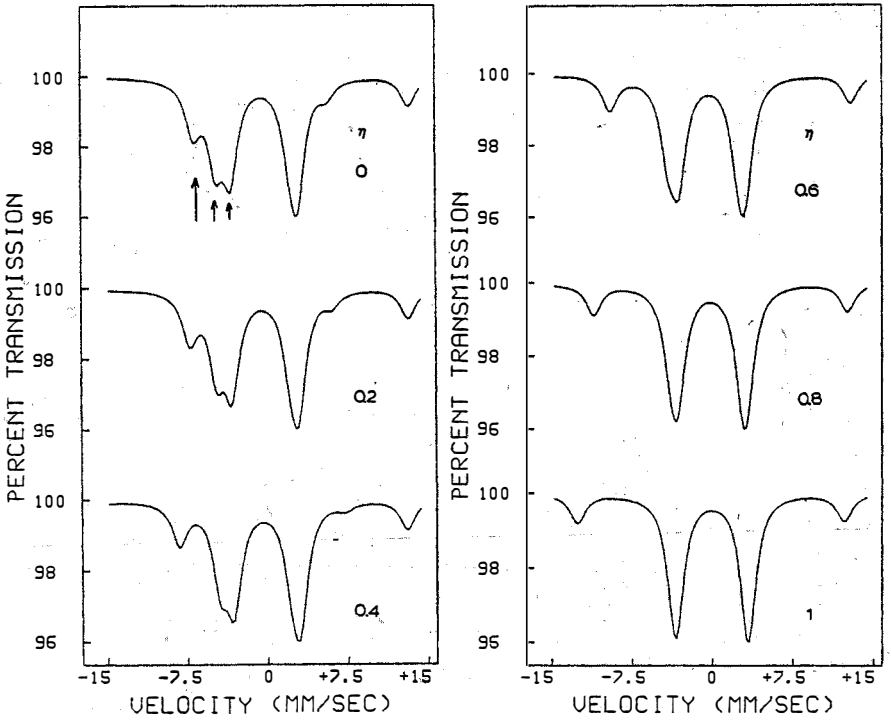

Fig. 7 η dependence of the ^{129}I electric quadrupole multiplet structure for a fixed value of $e^2Q_gV_{zz}$. Note that when $\eta = 0$, the spectra reveal a characteristic triplet structure (shown by arrows) on one of the main lines.

when $\eta = 1$ can this not be done because the pattern becomes completely symmetric and the sign of EFG remains no longer defined. In particular, when $\eta = 0$, one observes a characteristic triplet structure (shown by arrows) on one of the principal lines seen in the spectrum. There are primarily two types of spectra we shall encounter in our glass work, one where $\eta = 0$ and the other where $\eta = 0.8$ or so.

Chemical bonding information in this spectroscopy is best obtained by plotting the isomer shift as a function of quadrupole coupling as shown in Fig. 8. Detailed discussion of this plot appears elsewhere in the literature [28-30] and will not be given here. Different parts of this plot pertain to I present in different chemical states. Specifically, a onefold coordinate I site, as in I_2 dimer for example, resides along the line drawn due north-east on this plot. Note that the sign of the quadrupole coupling of such a onefold coordinated species is always negative, and this is a point we will return to later.

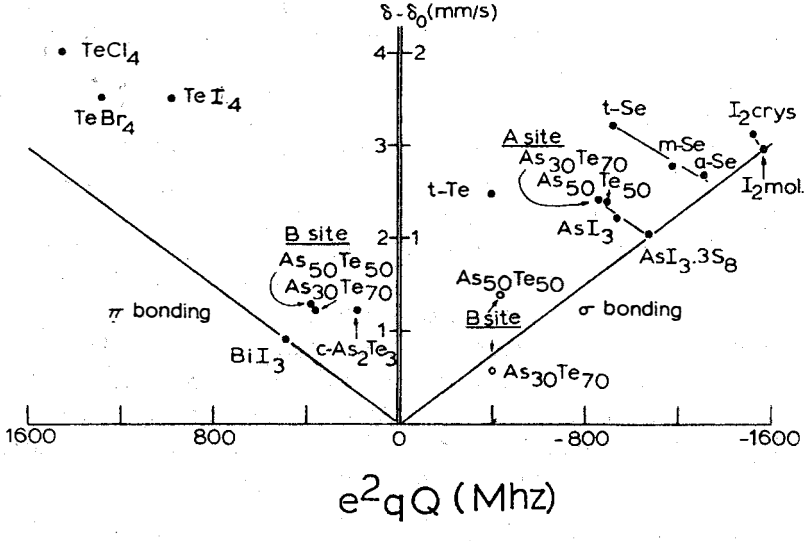

Fig. 8 Correlation of ^{129}I isomer shift with quadrupole coupling taken from ref. 29. Note that when I is onefold coordinated, the sign of the coupling is always negative.

Within the context of NQI as a probe of chalcogen chemistry, two central ideas need to be introduced at this stage. It is well known that the highly directional nature of bonds that chalcogens form arise due to the open p valence shell (s^2p^4). Specifically, the twofold coordination of these elements arise because two of the four p valence electrons enter in covalent bonds with two near-neighbors while the remaining two p electrons form the so-called nonbonding lone-pair electrons. Of course, the two s valence electrons can also participate in bonding by hybridization and their principal effect is to increase the chalcogen bond angle from 90° to about 102° as is found in the elemental chalcogens for example.

Because of the lack of cubic symmetry around a twofold coordinated Te site, one expects in general a large EFG. The magnitude and sign of this EFG can be inferred using an atomistic approach. Because of the local C_{2v} symmetry, the principal z axis of the EFG tensor is expected to lie along the lone-pair electron lobes, while the principal x and y axis to lie along the bonding orbitals. This distribution of the four p valence electrons requires the net EFG to be negative and of magnitude $\frac{4e}{5\langle r^3\rangle}$. For the case of crystalline Te, the sign of the EFG has been explicitly established [31], and it is indeed found to be negative as expected. We expect the sign of the EFG in general to be negative so long as Te is twofold coordinated as in the elemental chalcogens (p-S, a-Se).

Experiments on a wide variety of crystals have indicated the following general pattern: whenever the parent $^{129}Te^m$ atoms are twofold coordinated, as in the elemental chalcogens, the daughter ^{129}I is nominally onefold coordinated. This is inferred from the sign of the EFG which undergoes a change from being negative at a Te probe to positive at an I probe. We have suggested [24] that this pattern is the consequence of a bond rearrangement on account of a change in chemical valence. Specifically, the principal axis of the EFG rotates by 90° in going from a Te probe to an I probe (as shown in Fig. 9) as one of the Te π-bonds breaks and the other π-bond becomes an I-σ bond. Because all nuclear quadrupole moments are negative, the quadrupole couplings (e^2QV_{zz}) change sign from being positive at Te to negative at I. The positive sign of the EFG for onefold coordinated I site is best understood to arise, as in the case of an I_2 dimer, on account of σ bonding of p_z-like hole in the closed shell 5 s^2p^6 configuration.

Experiments also indicate that in instances when the parent Te atom has a coordination that is higher than twofold, such as threefold or distorted octahedral, the daughter I continues to remain π-bonded, i.e., the sign of the EFG remains unchanged and continues to remain negative [29]. Apparently, in such a case it is energetically unfavorable for more than one of the π-bonds to break to realize a onefold coordinated σ-bonded species.

There are two additional features of NQI parameters that serve as microscopic signatures of Te coordination. First, the ^{129}I quadrupole coupling of a π-bonded species is nearly half of a σ-bonded species for the same isomer shift. This is related to the fact that although each of the p_x, p_y, and p_z I-orbitals shields the 5s contact charge density by the same amount, the magnitude of EFG produced by a p_z orbital is twice that produced by a p_x or p_y orbital. Second, experiments reveal that in covalently-bonded networks, the ratio R of the ^{125}Te quadrupole coupling to the ^{129}I quadrupole coupling equals nearly 1/2, and is a point discussed elsewhere in detail [24].

To summarize, this spectroscopy makes accessible through the ^{129}I NQI parameters several tests of the Te parent coordination which derive from (a) sign of the ^{129}I $e^2Q_gV_{zz}$, (b) magnitude of ^{129}I isomer shift and $e^2Q_gV_{zz}$, and (c) ratio of $^{125}Te/^{129}I$ Quadrupole couplings, as discussed above.

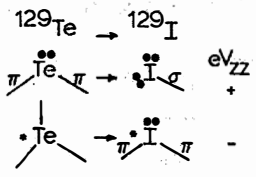

Fig. 9 Bonding configuration of ^{129}I daughter atoms formed from (a) twofold Te atoms, and (b) threefold Te atoms. The filled circle and asterisk designate lone-pair and antibonding electron states. Our usage of the terms π and σ bonds here differs from the usual chemical language in that these are defined in the principal axes of the EFG tensor of Te or I. See ref. 29 for additional details.

III. EXPERIMENTAL RESULTS ON $GeSe_2$ GLASS AND DISCUSSION

To probe the cation site in the glass of interest, we have examined ternary $(Ge_{0.99}Sn_{0.01})_xSe_{1-x}$ glasses prepared by melt quenching in water in the usual way [3]. Our approach is to examine the compositional evolution of the spectra as x approaches 1/3. For probing the chalcogen sites, we have chosen to look at ternary $GeSe_{2-x}Te_x$ glasses in a similar fashion, focussing on the nature of sites prevailing as x approaches 0. In what follows, we shall summarize results of these experiments which have been published elsewhere [23,30].

A. Ge Chemical Order

^{119}Sn Mossbauer spectra at selected compositions near $x = 1/3$ in the ternary $(Ge_{0.99}Sn_{0.01})_xSe_{1-x}$ are displayed in Fig. 10. The most striking result to emerge from these spectra is the presence of two types of Sn sites: a symmetric site A which shows a single line and an asymmetric site B which exhibits a quadrupole doublet (Table II). The site intensity ratio, $I_B/(I_A + I_B)$, increases with x in a manner that is sketched in Fig. 11. This figure also shows the T_g of the corresponding glasses for comparison which serves as a check of sample stoichiometry. The observed linewidths in the glasses Γ (full width at half maximum) = 0.93(3)mm/s

Table II ^{119}Sn isomer shift (δ) and quadrupole splitting (Δ) in indicated glass (g) and crystalline (c) samples. The shifts are quoted relative to $BaSnO_3$.

Sample		δ(mm/s)	Δ(mm/s)
g-$GeSe_2$	A	1.55 (3)	...
	B	3.20 (3)	2.13 (3)
c-$SnSe_2$		1.36 (2)	...
c-SnSe		3.31 (2)	0.74 (2)

are just as narrow as the ones seen in the $SnSe_2$ and SnSe crystals. This indicates that the sites (A,B) seen in the glasses are chemically well defined.

We identify site A in our spectra with Sn atoms that replace Ge in a symmetric tetrahedral $Ge(Se_{1/2})_4$ unit. The evidence to support this identification includes (i) the single-line nature of this site which is consistent with a vanishing EFG in a local tetrahedral coordination, (ii) the isomer shift of the single line (see Fig. 3 and Table II) which is characteristic of a Sn site that is geometrically and chemically tetrahedrally coordinated to four Se near-neighbors.

The dominant nature of site A at $x=1/3$ (shown by $I_B/I=0.16$ in Fig. 11) is in accord with results of Raman vibrational spectroscopy which reveal that $Ge(Se_{1/2})_4$ units comprise the principal

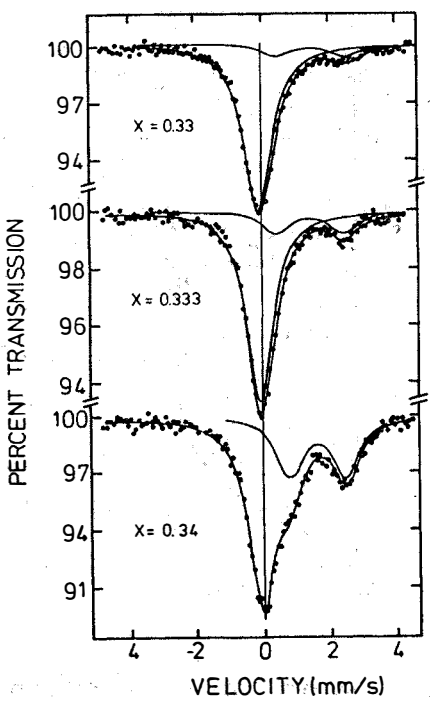

Fig. 10 ^{119}Sn spectra of indicated $(Ge_{0.99}Sn_{0.01})_xSe_{1-x}$ glasses showing the presence of two Sn sites: Site A is the intense single line near v = 0mm/s, while Site B is the quadrupole doublet centered at about +1.5mm/s. Figure is taken from ref. 26.

building block of a $GeSe_2$ glass. In our spectra, we identify site B with Sn atoms that replace one of the Ge sites in an ethane-like $Ge_2(Se_{1/2})_6$ unit. The evidence in support of this identification includes the doublet nature of this site which we believe results due to the locally asymmetric Sn coordination in such a cluster, and

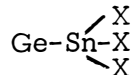

in which the broken tetrahedral symmetry causes a finite EFG and therefore a quadrupole splitting. Secondly, the I_B/I data of Fig. 11 shows that site B dominates as x approaches 2/5. This constitutes strong evidence in favor of the proposed identification because it has been shown by optical [32] and by chemical [33]

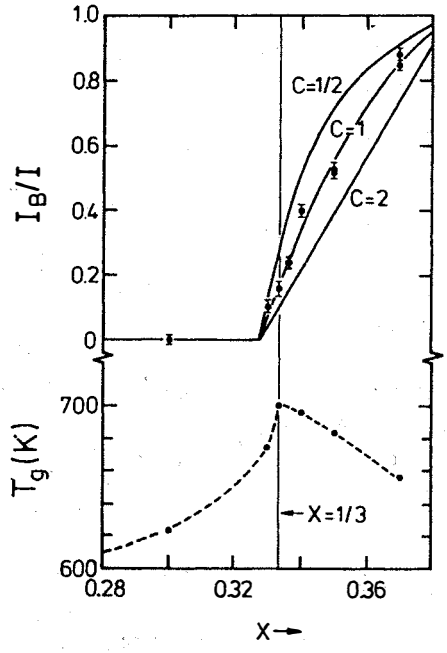

Fig. 11 Observed x-dependence of the site intensity ratio I_B/I and glass transitions (T_g) in melt quenched $(Ge_{0.99}Sn_{0.01})_xSe_{1-x}$ glasses. The parameter C describes chemical preference of Sn to choose A over B sites. C = 1 implies that Sn chooses to attach in A and local units randomly.

means that $Ge_2(Se_{1/2})_6$ ethane-like unit constitutes the principal building block of a Ge_2Se_3 glass. In our spectra, the observation of a finite intensity of site B at $x = 0.333$ constitutes, therefore, the first clear evidence for intrinsically broken Ge chemical order in a $GeSe_2$ glass. We have developed a model to relate the populations (N_A and N_B) of $Ge(Se_{1/2})_4$ and $Ge_2(Se_{1/2})_6$ units in the glass network to the measured Sn site occupations (intensities I_A and I_B) of these units. Let us suppose that I_B/I is a smooth function of x and takes on values of 0 and 1 at $x = x_o$ and $x = x_1$. Further, let us suppose that the intensities (I_A, I_B) depend on the populations (N_A, N_B) and on the chemical affinity $C = \exp[(E_B - E_A)/kT_g]$ of Sn atoms to attach themselves in respective Ge units. $E_B - E_A$ represents the bond energy difference in moving a Sn atom from a site B to a site A. On minimizing the free energy, one can show that

$$\frac{I_B}{I_A + I_B} = \frac{N_B}{C\,N_A/2 + N_B} = \frac{x - x_o}{C(x_1 - x)/2 + (x - x_o)} \,. \qquad (4)$$

The smooth curve through the data points in Fig. 11 is a fit to Eq. (4), and yields $C = 1.0$, $x_1 = 0.385(4)$. The value of $C = 1$ indicates that Sn atoms choose randomly the available Ge units, and further that I_B/I equals the fraction of Ge sites in ethane-like units of the network. We define the degree of broken order (DBO) in a $GeSe_2$ glass as the fraction of Ge sites in ethane-like units of the network, i.e., $2N_B/(N_A + 2N_B)$ and find its value to be 0.16(1).

The trend of an increase in the site intensity ratio I_B/I with x (Fig. 9), particularly in the composition range $x_o < x < 0.333$, where T_g of the glasses increases so rapidly, is a remarkable result. This trend is much too steep to be described by a model in which the chemical order breaking site B is identified with some Ge-Ge bonds that are formed at random in an ordered bond network. This is seen by comparing the observed slope $d(I_B/I)/dx$ at $x = 0.33$ of 32(2) [Fig. 11 and Eq. (4)] with the calculated slope $d(N_{Ge\text{-}Ge}/N)/dx$ of 18 describing the change in the fraction of Ge sites in Ge-Ge bonds at $x = 0.333$ in an ordered bond network. Indeed, as the number of Ge-Ge bonds at $x = 0.333$ increases (increased disorder), the slope $d(N_{Ge\text{-}Ge}/N)/dx$ can be shown to decrease from its maximum value of 18 to a minimum value of 4, for a completely random covalent network. This trend, on the other hand, is better described as reflecting a rapid growth in the fraction of Ge sites in $Ge_2(Se_{1/2})_6$ clusters with x. Such sites

correspond to Ge-Ge bonds. According to our data, the fraction $Ge_2(Se_{1/2})_6$ clusters, i.e., $N_B/(N_A + N_B)$, is predicted to vary nearly linearly with x (straight line corresponding to C = 2 in Fig. 9). This linear variation is expected to scale with the scattering strength of the $180cm^{-1}$ feature [shown in ref. 32 to be the benchmark of a $Ge_2(Se_{1/2})_6$ unit in Raman spectra of Ge_xSe_{1-x} glasses]. The overall picture of the network structure emerging from different types of measurements will be discussed in Section IV.

B. Se Chemical Order

Selected ^{129}I emission spectra of ternary $GeSe_{2-x}Te_x$ glasses [23,30] and the elemental chalcogens are displayed in Fig. 12. The central result to emerge from these spectra is that in glasses of $GeSe_{2-x}Te_x$ and $GeS_{2-x}Te_x$, even as x approaches 0, there are two inequivalent I sites, A and B. For example, as can be seen in Fig. 12, a qualitative improvement in the fit to a g-$GeSe_2$ spectrum results in going from a one-site to a two-site fit. The NQI parameters $e^2QV_{zz}^A$, $e^2QV_{zz}^B$, η^B, and η^A for $GeSe_{2-x}Te_x$ alloys are shown as a function of x in Fig. 13. These parameters were obtained by standard Mössbauer spectra analysis described in Section II.B, and for $x \rightarrow 0$, they are compared in Table III with the elemental solute parameters. Note that the sign of e^2qQ is negative at both A and B sites, suggesting that the parent Te site is twofold coordinated in each instance. There is compelling evidence that the two sites seen in the present glasses do not originate from a nuclear aftereffect, such as bond breaking following nuclear transmutation. To date, such an effect has not been observed in any metallic or semiconducting host. Our observation of a unique and static NQI in the elemental glasses (S, Se), see Fig. 12 and Table III, follows this pattern, and it strongly suggests the absence of a nuclear aftereffect in these semiconducting glasses.

Most recent workers have assumed that the atomic structure of chalcogenide glasses can be described in terms of a chemically ordered CRN as originally proposed by Zachariasen [1]. Our data provide the first direct evidence that this is not the case. Specifically, let us suppose that chalcogen sites are of two types, a chemically ordered site A bonded to two Ge atoms, and site B bonded to a Ge atom and a chlacogen atom. Let the probability that a Te atom occupies an A or B site be p^A or p^B, and let the branching probabilities that B site daughter I atoms will choose

to attach themselves to the Ge or chalcogen neighbors be f_G or f_C. Then, the probabilities $P_{G,C}$ that ^{129}I will be bonded to Ge or the chalcogen are given by

$$p_G = p^A + p^B f_G, \tag{5}$$

$$p_C = p^B f_C. \tag{6}$$

Returning to Table I, we see by comparison with the elemental chalcogen parameters (e_2QV_{zz}, η, and isomer shift) that for $x \to 0$, i.e., $GeSe_2$ (and also GeS_2), the B site definitely corresponds to an I-chalcogen bond. Further, we note by comparing

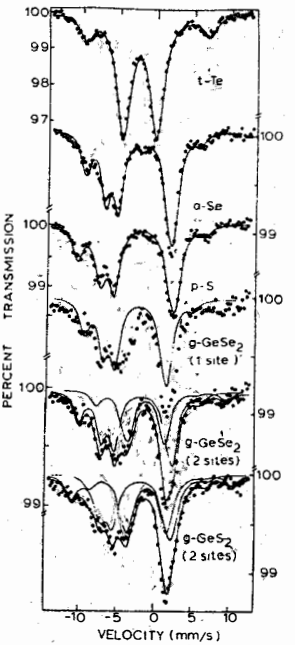

Fig. 12 ^{129}I emission spectra of indicated hosts taken from ref. 30. A noticeable improvement in the fit to the spectrum of g-$GeSe_2$ results in going from a one-site to a two-site fit.

A-site parameters in $GeSe_2$ with the A-site parameter in GeS_2 that these are really the same site, and identify it with an I-Ge bond. Regardless of the transmutational branching probabilities f_G and f_C, Eq. (6) tells us that there must be a substantial probability p^B of the type B Te sites in the glass, i.e., the chemical ordering must be intrinsically broken.

According to Fig. 13, $I_B(x) > I_A(x)$, i.e., $p_C(x) > p_G(x)$, at $x = 0$ and further $p_C(x)$, $e^2QV_{zz}^B$, and η^B all sharply change with increasing x, especially p_C which is already halved at $x = 0.2$. This suggests several interpretations of the chalcogen environments

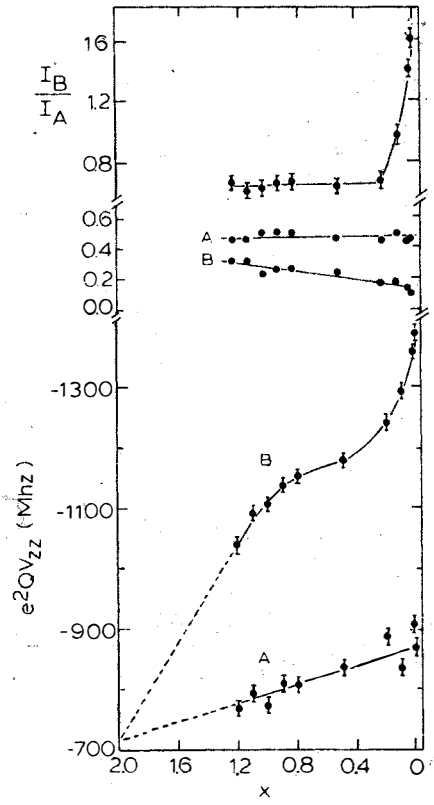

Fig. 13 The observed variation of the quadrupole couplings ($e^2Q_gV_{zz}$), intensity ratio I_B/I_A, and asymmetry parameter (η) for the two sites in g-$GeSe_{2-x}Te_x$ alloys (x) of the glass.

and the physical mechanism responsible for the transmutational branching ratio. Because $p_C(0) > p_G(0)$, we conclude that f_G/f_C is small and is probably close to zero, i.e., I prefers to form I-Se(S) rather than I-Ge bonds in the glass. This result is somewhat surprising, because according to Pauling [34] the ionic contribution to the heat of formation of I-Ge bonds should be almost 50 times greater than that of I-Se(S) bonds. We must remember, however, that these bonds are not formed in the vapor or in dilute solution. Instead, they are formed in the melt quenched glass which is 90% as dense as the crystal. In dense covalent networks the Van der Walls repulsive energy between nonbonded lone-pair electrons can be quite large, as is shown by the near equality of bonded and nonbonded interatomic spacings in elemental Se crystals. Thus, at B sites, I-Se(Se) bonds are formed in preference to I-Ge bonds, apparently because in the latter case, the repulsive or steric hindrance nonbonded I-Se(S) interactions overwhelm the ionic energy difference.

The rapid variation in the site intensity ratio displayed in Fig. 13 with x will be discussed in the next section in connection with the structure of $GeSe_2$ glass.

Table III ^{129}I quadrupole coupling (e^2QV_{zz}), asymmetry parameter (η), and isomer shift (δ) deduced from spectra of Fig. 1. δ is quoted relative to $Na^{129}I$.

Host	e^2QV_{zz}(MHz)	η	δ(mm/s)
t-Te	- 397 (2)	0.70 (1)	1.16 (1)
a-Se	- 1341 (10)	0.11 (2)	1.26 (4)
p-S	- 1453 (6)	0.13 (2)	1.26 (2)
$GeSe_2$ A	- 860 (12)	0.49 (6)	0.76 (3)
$GeSe_2$ B	- 1360 (9)	0.15 (6)	1.28 (4)
GeS_2 A	- 936 (15)	0.57 (6)	0.62 (4)
GeS_2 B	- 1432 (10)	0.25 (6)	1.29 (4)

IV. STRUCTURE OF $GeSe_2$ GLASS

The network structure of $GeSe_2$ has been the focus of previous Raman and diffraction measurements. In this section, we will show that the present Mossbauer results extend in a significant way the understanding of the morphological structure of this material as deduced from the previous investigations. We shall conclude by showing that the present experiments strongly suggest that $GeSe_2$ glass is an incompletely polymerized tetrahedral network, and is better described in terms of a heterogeneous microstructure consisting of clusters.

A. Diffraction Experiment

Chemically specific diffraction experiments [35] utilizing EXAFS of the Ge K edge and Se K edge in glassy and crystalline $GeSe_2$ have been observed. The interference function analysis indicates that on an average Ge and Se atoms are coordinated respectively to four Se and two Ge near-neighbors in accord with the 8-N coordination rule. These experiments make it plausible to visualize the $GeSe_2$ glass network in analogy to the crystal to consist predominantly of $Ge(Se_{1/2})_4$ tetrahedral building blocks.

It also appears that the tetrahedral units in the glass, as in the high temperature crystalline phase of $GeSe_2$, may be present in a layered morphology. Both x-ray [36] and neutron [37] structure factor of g-$GeSe_2$ reveal an anomalous sharp diffraction peak at $k = 1.1\ \text{Å}^{-1}$ (see Fig. 14). Anomalous x-ray scattering techniques [38] using a syncrhrotron source have further shown that the peak at $k = 1.1\ \text{Å}^{-1}$ corresponds to Ge-Ge correlation. Because this correlation translates into a real space distance of about 6Å, which also happens to be the Ge-Ge interlayer distance in β-$GeSe_2$ [39], it appears plausible that this peak may signify the presence of medium range order in a network which consists of locally layered like structures.

Neutron diffuse scattering experiments on $GeSe_2$ glass and liquid show certain common features. Surprisingly, both structure factors display the anomalous sharp first diffraction peak at $k = 1.1\ \text{Å}^{-1}$ alluded to above, albeit the width of this peak being broader in the liquid phase. Furthermore, Raman spectra of liquid and glassy $GeSe_2$ both display [40] the so-called A_1 companion mode. This mode is generally taken to be signature of medium-range order and will be discussed in more detail next. To summarize, characteristic features of both Raman and diffraction

experiments, thus, clearly indicate that the medium-range structure of the glass bears some relationship to that of the liquid. It is plausible to imagine that characteristic molecular fragments having a local layered-like arrangement of tetrahedral units persist in both these phases. After all, the glass does evolve from the liquid and is, in fact, the supercooled liquid.

B. Vibrational Spectroscopy

Direct confirmation of the tetrahedral nature of the principal building block of a $GeSe_2$ glass network has emerged by decoding Raman scattering [41,42] and IR reflectance spectra [43]. These spectra reveal several sharp vibrational modes. Several of these modes have been positively identified as the normal modes of nearly decoupled tetrahedral $Ge(Se_{1/2})_4$ units in g-$GeSe_2$. Variation of mode strengths with glass composition in Ge_xSe_{1-x} glasses, measurements of depolarization ratios [42], and, finally, comparison of observed mode frequencies with theo-

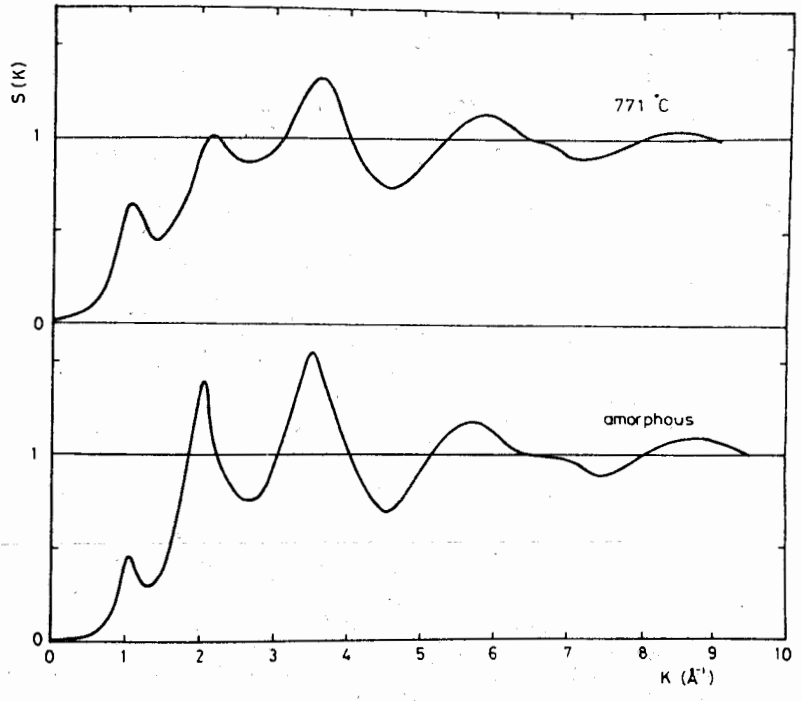

Fig. 14 Neutron scattering structure factor of liquid and glass $GeSe_2$ (taken from ref. 37) showing the first anomalous sharp peak at $k = 1.1\ Å^{-1}$.

retical estimates of one phonon density of states in model clusters [45] have served to confirm the microscopic origin of the modes. Specifically, in the Raman spectra of g-$GeSe_2$ (see Fig. 15), the sharp mode at 200 cm^{-1} and the broad one at 304 cm^{-1} are identified as the A_1 symmetric breathing mode and the F_2 high frequency scissor mode of a $Ge(Se_{1/2})_4$ tetrahedral unit. In the spectrum, there are two surprises, however, and these include (a) a weak mode at 180 cm^{-1} which appears as a shoulder to the A_1 mode, and (b) a narrow and intense mode at 210 cm^{-1}, usually labelled as A_1^c, the companion of the A_1 mode. The microscopic origin of the 180 cm^{-1} is identified as the normal mode of non-tetrahedral species, specifically A_{1g} mode [42] of an ethane-like $Ge(Se_{1/2})_6$ cluster. The origin of the A_1^c mode, on the other hand, has been the subject of some controversy. Nemanich and Solin [1] were the first to emphasize that the rapid variation of the A_1^c mode strength in the Se-rich ($x > 1/3$) phase of the $Ge_{1-x}Se_x$ binary requires the presence of large clusters in the glass. In their model, their clusters were described to be 12-atom rings of Ge_6Se_6 which

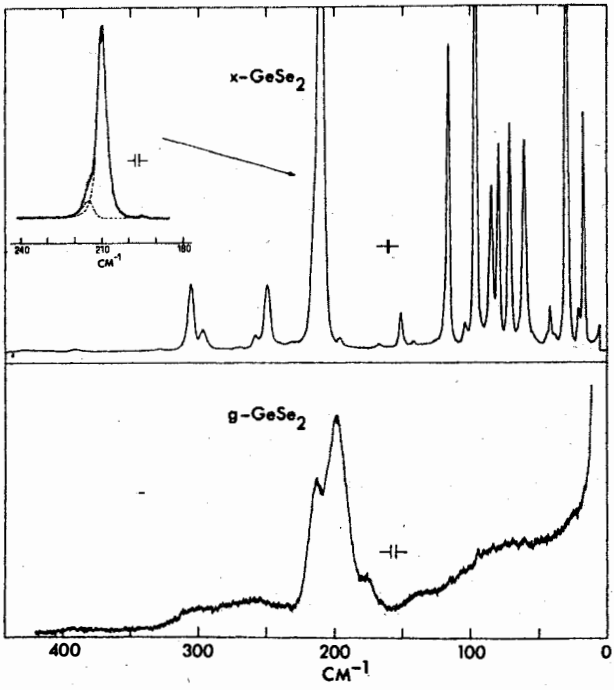

Fig. 15 Raman spectrum of crystalline and glassy $GeSe_2$ taken from ref. 46.

are embedded in a perfectly chemically ordered network (Fig. 16a). Bridenbaugh et al. [46], on the other hand, proposed that chemical order is intrinsically broken in the stoichiometric glass. They suggested that two kinds of partially polymerized clusters are present which are either cation-rich or chalcogen-rich. The latter were proposed to be raft-like fragments of the high temperature crystalline form, and were laterally bordered by chalcogen-chalcogen bonds (Fig. 16b). These workers identified the A_1^C mode as a Ge-Se stretch mode localized at the edges of this chalcogen-rich cluster. This particular interpretation of the A_1^C mode is now supported by the recent photostructural transformation [2] studies and vibrational density of states calculations [45], and also by our Mössbauer spectroscopy results [2,23,30,48] which will be discussed next.

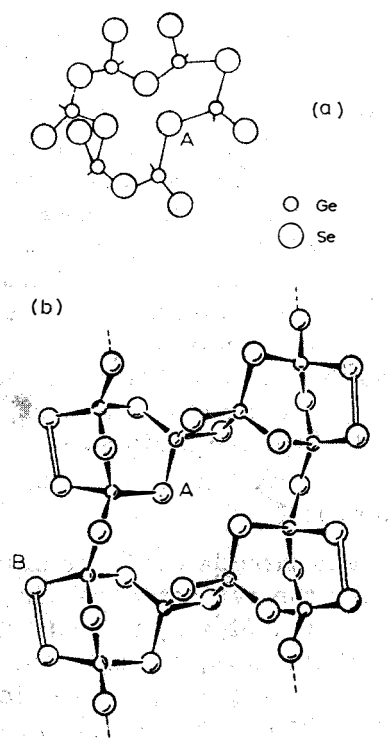

Fig. 16 Elements of medium-range order in g-$Ge-Se_2$ according to (a) CRN model, and (b) outrigger-raft model; (a) shows a Ge_6Se_6 ring cluster providing for one A site, while (b) shows a Ge_6Se_{14} outrigger-raft cluster providing for two chemically inequivalent A and B Se sites.

The heterogeneous character of Ge(Se or S)$_2$ glass network has been beautifully illustrated in a series of recent pressure dependent Raman [49] and optical absorption edge shift [50] experiments. In the Raman experiments on g-$GeSe_2$ for example, Murase et al. observe the scattering strength of the A_1^c mode extrapolate to zero at a pressure of 48 kbar. Apparently, the molecular clusters prevailing at ambient pressure coalesce through cluster surface reconstruction upon application of pressure. The high pressure phase of g-$GeSe_2$ may represent the second clear example of a Zachariasen network, the first example being the ternary glass $Ge_{0.65}Sn_{0.35}Se_2$, as illustrated by the Mössbauer experiments of Stevens et al. [48].

C. Mössbauer Spectroscopy

(i) Degree of Broken Chemical Order on Cation and Anion Sites Compared

Both the ^{119}Sn and ^{129}I experimental results on $(Ge_{0.99}Sn_{0.01})$, Se_{1-x}, and $GeSe_{2-x}Te_x$ glasses, which were presented in Section III, provide conclusive evidence for the existence of symmetry breaking B sites in $GeSe_2$. It is instructive to inquire if the degree to which the chemical order is broken at cation sites and anion sites bears any relationship to each other. This requires that we establish explicitly the ratio of occupation probability of the probe atoms (Sn or Te) to attach themselves in the two chemically inequivalent (A,B) sites of the network. We have already demonstrated in Section III that for the case of Sn, probe atoms randomly select A and B sites of the network. This led us to conclude that the fraction of nontetrahedral Ge sites present in $GeSe_2$ network is 0.16(1).

Our ^{129}I experiments provide evidence of a high selectivity of the Te atoms to replace the symmetry breaking B sites over the A sites, and this is seen by analyzing the variation of the site intensity ratio $I_B(x)/I_A(x)$ which rapidly increases in the composition range $0 < x < 0.1$. We have built a statistical model [30] in which $GeSe_{2-x}Te_x$ alloy glasses for $x < 0.1$ are visualized as made up of strings consisting of single chalcogen strings: Ge-Se-Ge and Ge-Te-Ge, and double chalcogen strings: Ge-Se-Se-Ge, Ge-Se-Te-Ge, and Ge-Te-Te-Ge. The crosslinking of the strings at Ge insures that 8-N coordination rule is satisfied, i.e., Ge is always fourfold and the chalcogen always twofold coordinated. By assigning characteristic energies to these strings

and minimizing the free energy of the stringed network, we have projected (Fig. 17) the population ratio R of Ge-Se-Te-Ge strings (B sites) to Ge-Te-Ge strings (A sites) as a function of x. The calculations show that in the Se-rich phase of the present ternary this ratio depends on two parameters ρ and β. We define ρ as the population ratio of all double chalcogen strings to all single chalcogen strings, while β as the probability ratio of Te to select B sites over A sites. We find from Fig. 17 that to reproduce the rapid variation of $I_B/I_A(x)$, the parameters $\rho \leq 1/16$ and $\beta \geq 13$. The finite value of ρ indicates that the stringed network is chalcogen rich, and is characterized by a stoichiometry of $GeSe_2(1+2\rho)/[(1+2\rho)/(1+\rho)]$. Specifically, the value of $\rho \leq 1/16$ implies that the stringed network has on average stoichiometry that is Se poorer than $Ge_{17}Se_{36}$. The value of $\beta \geq 13$, on the other hand, shows that there exists a high preference for Te to populate B sites over the A sites.

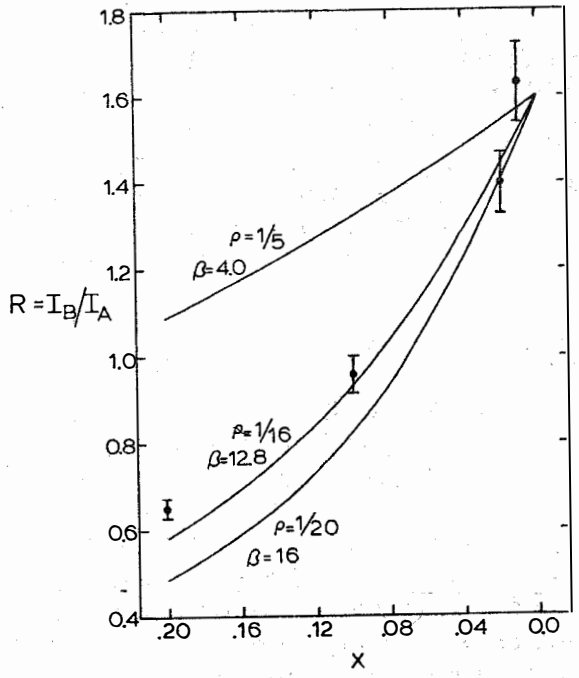

Fig. 17 Plot of R = Ge-Se-Te-Ge strings to Ge-Te-Ge strings in $GeSe_{2-x}Te_x$ glasses as a function of x. The parameters $\rho = M/N$ = #double chalcogen strings/#single chalcogen strings; and β describes the chemical preference of Te to select B sites over A sites. The data points are taken from ref. 23.

It becomes transparent from the above analysis that one can describe the $GeSe_2$ glass to be phase-separated into a Se-rich stringed cluster of $Ge_{17}Se_{36}$ stoichiometry and a compensating Ge-rich cluster of Ge_2Se_3 stoichiometry as follows:

$$Ge_{17}Se_{36} + 2\ Ge_2Se_3 + 21\ GeSe_2 \qquad (7)$$

then an upper limit to the degree of broken Ge chemical order would be $4/(4+17) = 0.19$. Note that all Ge sites in the ethane-like cluster possess locally a nontetrahedral symmetry while those in the Se-rich cluster all possess locally tetrahedral symmetry. We find that this value of $N_B/N = 0.19$ is very compatible with the value of 0.16(1) that we deduced earlier from our ^{119}Sn experiments directly. These results are particularly striking because these have been obtained by two completely independent probes of the chemical order of $GeSe_2$ glass.

(ii) B Sites are not Defects in a CRN

It is conceptually helpful at this stage to recall general features of the Mössbauer results that rule against assigning B sites to isolated bonding defects (homopolar bonds) frozen in a CRN which consists predominantly of heteropolar bonds. In Section IIIA and B, we indicated that the relative population of B sites seen in both the ^{119}Sn and ^{129}I experiments vary rapidly and systematically with glass composition. This rapid variation requires, on account of the law of mass action, that these sites be formed in a cluster.

If B sites were point defects in a CRN, one would expect their thermal population to change with degree of annealing of the network, as defects normally do in a crystal. Guided by these considerations, we performed ^{119}Sn experiments on melt quenched $Ge_{0.99}Sn_{0.01}Se_2$ and $Ge_{0.99}Sn_{0.01}S_2$ glasses in their virgin (as quenched in water) state and annealed state. The annealed state was achieved by taking the virgin sample to the glass transition temperature for the order of tens of minutes and thereafter cooling to room temperature slowly (over a period lasting 10-15 minutes). The spectra revealed no measurable change in the DBO on account of this thermal annealing. As the temperature of annealing exceeded, the crystallization temperature of the glass, first order changes in the spectra could be understood in terms of crystallization of specific phases. These thermal annealing studies reinforce the view that the B sites seen in our spectra form an intrinsic part of the glass network.

(iii) Sites Intensity Ratio: Signature of Cluster Size

The proposal of outrigger-raft [46] for the structure of $GeSe_2$ glass has several attractive features that provide a way to understand the Mössbauer results. In this cluster, the symmetry breaking Ge-Se-Se-Ge strings (providing a source of ^{129}I B sites) reside on the outer edges of the cluster in contrast to a Ge-Se-Ge strings (source of ^{129}I A sites) that occur in the interior of the cluster. One may understand the high selectivity ($\beta \geq 13$) of the oversize anion probe (Te) to choose B sites over A sites in terms of a strain mediated process. Apparently, either in the melt, or in the process of quenching, Se replacement by Te in the interior of the cluster must induce sufficient strain to drive the oversized impurity to cluster surfaces in much the same way that impurities segregate at grain boundaries in polycrystalline materials.

The outrigger-raft model proposal [46] consisting of two corner-sharing chains, on the other hand, is quantitatively incompatible with the degree of broken chemical order deduced from the present Mossbauer experiments. This is seen by writing the stoichiometry of the two-chain raft as Ge_6Se_{14}, which requires that the following stoichiometric relation exist for cluster phase separation

$$Ge_6Se_{14} + 2\ Ge_2Se_3 = 10\ GeSe_2\ . \qquad (8)$$

The above equation requires that the degree of broken Ge-chemical order be $4/(4+10) = 0.40$. Inspection of the crystal structure of g-$GeSe_2$ reveals that there are specific lateral dimensions (along b axis) at which bordering by Se-Se bonds can be invoked to produce characteristic clusters of progressively reduced Se excess. One such cluster of $Ge_{22}Se_{46}$ stoichiometry (Fig. 18) consisting of six corner-sharing chains laterally, provides, according to our data, an excellent candidate to be the Se-rich cluster of $GeSe_2$ glass. The stoichiometry of the reconstructed fragment requires that we write the molecular phase separation as

$$26\ GeSe_2 = Ge_{22}Se_{46} + 2\ Ge_2Se_3. \qquad (9)$$

According to this equation, the broken Ge chemical order is expected to be 0.154, and it compares favorably to the value of 0.16(1) deduced from our ^{119}Sn experiments.

D. Correlation of Raman and Mössbauer Results

It is instructive to inquire at this stage if one can quantitatively understand features of broken chemical order from the Raman

and Mössbauer spectra of $GeSe_2$ glass in terms of the idea of molecular phase separation into a large Se-rich and a small Ge-rich cluster. In Raman spectroscopy, scattering cross sections can vary by order of magnitude from one vibrational mode to another. This, of course, is in sharp contrast to Mössbauer spectroscopy where the absorption cross section ($n\sigma_o f$; n = area density of resonant nuclei, σ_o = nuclear resonant cross section, and f = recoil free fraction) is nearly site chemistry independent, particularly at low temperatures, where f-factors tend to saturate. Furthermore, while scattering strengths in Raman spectroscopy scale as the number of bonds, resonant absorption signal in Mössbauer spectroscopy scales as the number (n) of sites. The molecular phase separation of a $GeSe_2$ glass described by Eq. (9) requires that there be two homopolar Ge-Ge bonds for every 100 heteropolar Ge-Se ones. If one assumes a priori that the Raman scattering cross section of a Ge-Se bond and a Ge-Ge bond is the same, then one finds surprisingly that the observed scattering strength [1] ratio of the 180 cm^{-1} (A_{1g} ethane-like) to the 202 cm^{-1} (A_1 mode) of 2% or so (Fig. 15) is in excellent accord with the present model of molecular phase separation.

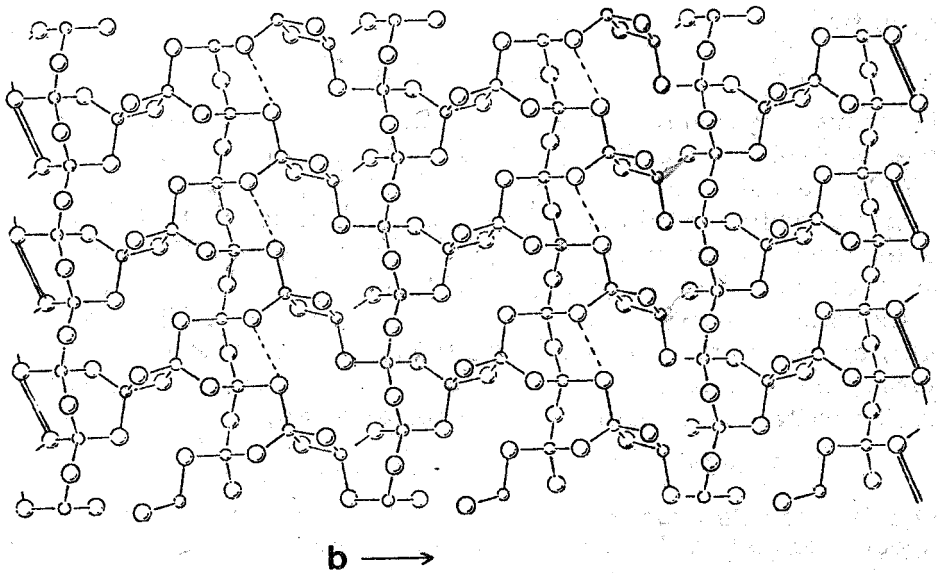

Fig. 18 Crystal structure of β-$GeSe_2$ showing provision for laterally terminating the network to form outrigger-rafts containing 2,4, or 6 chains. As the number of chains increases, the Se excess of the rafts decreases and the anticipated broken chemical order reduces.

V. CONCLUDING REMARKS

We conclude with several general comments central to the application of Mössbauer spectroscopy as a probe of structure of network glasses. These comments are meant to serve as a guide to the scope and limitations of the present approach.

(i) Our use of Sn and Te impurity atoms as probes of Ge and Se sites (chemical order) in a $GeSe_2$ glass is contingent upon the probe atoms replacing their lighter isovalent counterparts in the host. If supercooled melts of $SnSe_2/GeSe_2$ and $GeSe_2/GeTe_2$ display a pronounced tendency to phase separate, then clearly the present approach will not serve its intended purpose. As far as we can tell, the evidence at our disposal, from thermodynamics and microscopic measurements [18], strongly suggests that indicated melts when water quenched yield homogeneous single phase bulk glasses that display a single glass transition temperature [47]. This transition, furthermore, is found to monotomically and nonlinearly decrease with composition. The reader is referred to the extensive discussion of this point in ref. [48].

In general, the validity of the present method as a probe of the morphological structure of network glasses requires that probe atoms such as Sn, Sb and Te replace their lighter isovalents Ge, As, Se in host chalcogenide networks.

(ii) Because of the open 5p shell in the Mössbauer probe atoms Sn, Sb, and Te, the EFG parameters and contact charge density in dense covalent networks can be expected to be largely determined by the distribution of valence electrons. This has the important consequence that the nuclear hyperfine structure is largely determined by nearest neighbor coordination shell. It is for this reason that observation of chemically inequivalent sites in the spectra establishes aspects of short-range order of a glass network.

(iii) The use of oversized atoms can be a distinct advantage to probe network chemical order or the lack of it, for it may provide the driving mechanism that determines the high selectivity of probe atoms to populate one or more of the inequivalent sites (A, B) of a network. If this turns out to be the case, this, of course, needs to be established. This selectivity could be an asset, particularly if probe atoms have affinity for replacing the symmetry breaking sites of a network. The intensity enhancement of the B sites in ^{129}I emission spectra of $GeSe_2$ glass, where $I_B > I_A$ is a spectacular case in point.

(iv) Compositional variation of site intensity ratios I_B/I_A in the ^{129}I emission spectroscopy and in the ^{119}Sn absorption spectroscopy provides important clues on elements of medium-range order of the network. We have shown specifically that the rapid variation of these site intensity ratios with x requires, because of statistical considerations, that clustering must occur in the networks. These structure results are nicely complemented by recent Raman and optical absorption edge measurements [49,50].

(v) Measurements of T-dependence of Mössbauer recoil-free fraction f(T) can provide valuable insights in the low frequency one phonon density of states in glasses. We have, for example, studied in detail the f(T) of the two ^{119}Sn A and B sites in GeS_2 glass and find that the characteristic vibrational frequency of the tetrahedral A sites falls in the domain of the low frequency F_2 scissor mode of tetrahedral $Sn(S_{1/2})_4$ units seen in Raman vibrational spectroscopy. Aspects of this chemically specific vibrational spectroscopy of glasses remain to be explored and these will complement results of IR and Raman spectroscopy on these materials. A more general, and in some sense more elaborate, method of studying vibrational excitations in glasses make use of Rayleigh scattering of Mössbauer resonant radiation and this method has been discussed in ref. [51].

(vi) Because of the high sensitivity of the present method to aspects of broken chemical order, it is of interest to inquire what, if any, is the role of sample preparation on the microstructure of a network glass. Although such questions have been surely asked in the past, answers on a quantitative level have been hard to come by. Using the present approach, however, we are now in a position to quantitatively compare the DBO in a melt quenched glass with that of an amorphous film of the same composition prepared by vapor deposition, such as evaporation or sputtering. Preliminary experiments indicate that evaporated $GeSe_2$ films do, indeed, exhibit a substantially higher degree of broken order than a melt quenched glass. More significantly, the annealing kinetics of DBO in vapor deposited films are notoriously slow. These results will be discussed in forthcoming publications.

ACKNOWLEDGEMENTS

During the course of work on glasses I have benefitted greatly from collaboration and discussions with John deNeufville, Stan Ovshinsky, Jim Phillips, Peter Suranyi, Michael Tenhover,

and Mark Van Rossum. In addition, I have also had the pleasure to work closely with Wayne Bresser, Jeff Grothaus, Mark Stevens, George Lemon and Dave Ruffolo, all of whom have actively participated in this research effort on glasses at the University of Cincinnati. I acknowledge their contribution as well. This effort is currently supported by National Science Foundation Grant No. DMR-82-17514.

REFERENCES

1. W.H. Zachariasen, J. Am. Chem. Soc. 54, 3841(1932); M.F. Thorpe in Vibration Spectroscopy of Molecular Solids, edited by S. Bratos and R.M. Pick, Plenum, New York (1979), p. 341; R.J. Nemanich, G.A.N. Connell, T.M. Hayes and R.A. Street, Phys. Rev. B 18, 6900(1980).
2. J.E. Griffiths, G.P. Espinosa, J.P. Remeika and J.C. Phillips, Solid State Commun. 40, 1077(1981); Phys. Rev. B 25, 1272(1982); K. Murase, T. Fukunaga, Y. Tanaka, K. Yakushiji and I. Yunoki, Physica 117B and 118B, 962(1983).
3. P. Boolchand, J. Grothaus, W.J. Bresser and P. Suranyi, Phys. Rev. B 25, 2975(1982); P. Boolchand, J. Grothaus and J.C. Phillips, Solid State Commun. 45, 183(1983).
4. S.R. Ovshinsky, AIP Conference Proceedings 31, 67(1976).
5. J.P. deNeufville (private communication); also see J. Noncryst. Solids 8-10, 85(1972).
6. J.C. Phillips, J. Noncryst. Solids 34, 153(1979); 43, 37 (1981).
7. A. Feltz and H. Aust, J. Noncryst. Solids 51, 395(1982).
8. R.L. Mossbauer, Z. Physik 151, 124(1958); Naturwissenschaften 45, 538(1958). For review articles on the Mössbauer method used as a probe of glasses, see P.P. Seregin, A.R. Regel, A.A. Andreev and F.S. Nasredinov, Phys. Stat. Sol. (a) 74, 373(1982) and W. Müller-Warmuth and H. Eckert, Phys. Reports 88, 93(1982).
9. An excellent overview of the metallic glass systems investigated can be obtained in Proceedings of the International Conference on Amorphous Systems investigated by Nuclear Methods Balatoonfured, Hungary, September 1981, published in J. Nucl. Instrum. Methods 199, (1982). A review of the early oxide work has been given by C.R. Kurkjian, J. Noncryst. Solids 3, 157(1970).

10. A.C. Wright and A.J. Leadbetter, Phy. and Chem. of Glasses 17, 122(1976).
11. M.H. Brodsky in Amorphous Semiconductors, Topics in Applied Physics, Springer Verlag, (1979), vol. 37.
12. L. Ley, M. Cardona and R.A. Pollak in Photoemission in Solid II, Topics in Applied Physics, Springer Verlag, (1979), vol. 27, p. 11.
13. P.J. Bray, F. Bucholtz, A.E. Geissberger and I.A. Harris, Nucl. Instrum. Methods 199, 1(1982).
14. M. Rubinstein and P.C. Taylor, Phys. Rev. B 9, 4258(1974); also see J. Szeftel and H. Alloul, Phys. Rev. Lett. 42, 1691(1979); J. Szeftel, Phil. Mag. 43, 549(1981).
15. The Mossbauer effect of the 13.3keV x-ray in ^{73}Ge first observed by Raghavan and L. Pfeiffer, Phys. Rev. Lett. 32, 512(1974) has a natural linewidth of 6.98×10^{-3}mm/s. This extremely narrow resonance is hard to observe in well-ordered crystals because of inhomogeneous line broadening. In glasses this resonance is expected to have little use.
16. N.N. Greenwood and T.C. Gibb, Mössbauer Spectroscopy, Chapman and Hall Ltd., London, (1971); G.K. Shenoy and F.E. Wagner, Mössbauer Isomer Shifts, North Holland, (1978).
17. G. Weyer, B.I. Deutch, A. Nylandsted-Larsen, J.U. Anderston and H.L. Nielsen, J. Phys. 35, 6-297(1974); also see J.W. Peterson et al. Phys. Rev. B 21, 4292(1980); D.L. Williamson and S.K. Deb, J. Appl. Phys. 54, 2588(1983).
18. P. Boolchand and M. Stevens, Phys. Rev. B 29, 1(1984).
19. P.A. Flinn in Mössbauer Isomer Shifts, North Holland, (1978), p. 595; also see J.D. Donaldson and B.J. Senior, J. Inorg. Nucl. Chem. 31, 881(1969).
20. R.M. Sternheimer, Phys. Rev. 84, 244(1951); 95, 736(1954).
21. G. Czjzek, J. Fink, F. Gotz, H. Schmidt, J.M.D. Coey, J.P. Rebouillat and A. Lienard, Phys. Rev. B 23, 2513 (1981).
22. A. Coker, T. Lee and T.P. Das, Phys. Rev. B 13, 55(1976); 22, 2968(1980); 22, 2976(1980).
23. W.J Bresser, P. Boolchand, P. Suranyi and J.P. deNeufville, Phys. Rev. Lett. 46, 1689(1981); P. Boolchand, W. Bresser and G.J. Ehrhart, Phys. Rev. B 23, 3669(1981).
24. C.S. Kim and P. Boolchand, Phys. Rev. B 19, 3187(1979).

25. Sputtered amorphous films GeS, GeSe and GeTe have been studied by ion implanting $^{129}Te^{m}$ atoms and recording the ^{129}I emission spectrum of such targets by P. Boolchand et al., using the isotope separator at Leuven University, Belgium.
26. P. Boolchand, W.J. Bresser, P. Suranyi and J.P. deNeufville, Nucl. Instrum. Methods 199, 295(1982).
27. More precisely, the isomershift of NaI^{129} is taken to be +0.08(3)mm/s with respect to the closed shell configuration I. See ref. 28.
28. H. deWaard in Mössbauer Effect Data Index, edited by J.G. Stevens and V.E. Stevens, Plenum Press, N.Y., (1975), p. 447. (Covers 1973 literature.)
29. P. Boolchand, W.J. Bresser and M. Tenhover, Phys. Rev. B 25, 2971(1982).
30. W.J. Bresser, P. Boolchand, P. Suranyi, J.P. deNeufville and J.G. Hernandez, Phys. Rev. B, to be published.
31. P. Boolchand, B.L. Robinson and S. Jha, Phys. Rev. B 2, 3463(1970).
32. G. Lucovsky, R.J. Nemanich and F.L. Galeener, in Proceedings of the Seventh International Conference on Amorphous and Liquid Semiconductors, edited by W.E. Spear, Edinburgh, Scotland, (1977), p. 125.
33. A. Feltz, K. Zickmuller and G. Pfaff, in Proceedings of the Seventh International Conference on Amorphous and Liquid Semiconductors, edited by W.E. Spear, Edinburgh, Scotland, (1977), p. 133.
34. L. Pauling, The Nature of the Chemical Bond, Cornell University Press, Ithaca, (1960).
35. D.E. Sayers, F.W. Lyttle and E.A. Stern, in Proceedings of the Fifth International Conference on Amorphous and Liquid Semiconductors, edited by J. Stuke and W. Brenig, Taylor and Francis Ltd., London, (1974), p. 403.
36. L. Cervinka and A. Hruby, in Proceedings of the Fifth International Conference on Amorphous and Liquid Semiconductors, edited by J. Stuke and W. Brenig, Taylor and Francis Ltd., London, (1974), p. 431; also see L.E. Busse and S.R. Nagel, Phys. Rev. Lett. 47, 1848(1981).
37. O. Uemura, Y. Sagara and T. Satow, Phys. Stat. Solid A 26, 99(1974); J. Noncryst. Solids 33, 71(1979).
38. P.H. Fuoss, P. Eisenberger, W. K. Warburton and A. Bienenstock, Phys. Rev. Lett. 46, 1537(1981).

39. G. Dittmar and H. Schafer, Acta. Cryst. B 31, 2060(1975).
40. J.R. Magaha and J.S. Lannin, J. Noncryst. Solids 59-60, 1055(1983).
41. P. Tronc, M. Bensoussan, A. Brenac and C. Sebenne, Phys. Rev. B 8, 5947(1973); G. Lucovsky, J.P. deNeufville and F.L. Galeener, Phys. Rev. B 9, 1591(1974).
42. G. Lucovsky, F.L. Galeener, R.H. Geils and R.C. Keezer, in Proceedings of the Symposium on the Structure of Non-crystalline Materials, Cambridge, U.K., edited by P.H. Gaskell, Taylor and Francis Ltd., London, (1977), p. 127.
43. G. Lucovsky, R.C. Keezer, R.H. Geils and H.A. Six, Phys. Rev. B 10, 5134(1974).
44. R.J. Nemanich, S.A. Solin and G. Lucovsky, Solid State Commun. 21, 73(1977).
45. J.A. Aronovitz, J.R. Banavar, M.A. Marcus and J.C. Phillips, Phys. Rev. B 28, 4454(1983); T. Fukunaga, Ph.D. thesis (unpublished), Osaka University (1982).
46. P.M. Bridenbaugh, G.P. Espinosa, J.E. Griffiths, J.C. Phillips and J.P. Remeika, Phys. Rev. B 20, 4140(1979).
47. D.J. Sarrach, J.P. deNeufville, and W.L. Hayworth, J. Noncryst. Solids 22, 245(1976).
48. M. Stevens, J. Grothaus, P. Boolchand and J.G. Hernandez, Solid State Commun. 47, 199(1983); J.C. Phillips, ibid. 47, 203(1983).
49. T. Fukunaga, Proceedings of Optical Effects in Amorphous Semiconductors, Snowbird, Utah, August 1984; K. Murase and T. Fukunaga, 17th International Conference on Physics of Semiconductors, San Francisco, California, August 1984.
50. B. Weinstein and M.L. Slade, Proceedings of Optical Effects in Amorphous Semiconductors, Snowbird, Utah, August 1984; B. Weinstein et al., Phys. Rev. B 25, 781 (1982).
51. G. Alebenese and A. Deriu, Riv. Nuovo Cimento 2, 1(1979).